MODELING AND EXPERIMENTAL EVALUATION OF GEOMETRY AND WALL THICKNESS ON THE DYNAMIC PERFORMANCE OF SILICONE-BASED SOFT PNEUMATIC ACTUATOR

Muhammad Haziq Isham[a], Nur Safwati Mohd Nor[a]*, Muhammad Sunny Nazeer[b]

[a]Faculty of Mechanical Engineering, Universiti Teknologi Malaysia, 81310 UTM Johor Bahru, Johor, Malaysia.
[b]Department of Mechanical Engineering, National University of Singapore, Singapore 117575, Singapore.

*Corresponding email: nursafwati@utm.my

Article history
Received
15th August 2025
Revised
20th November 2025
Accepted
21st November 2025
Published
1st December 2025

ABSTRACT

This paper presents the design, fabrication, and testing of a pneumatic actuator using silicone rubber. The study addressed the need for adaptable, flexible actuators in soft robotics applications. Single and multi-chamber designs are created using SolidWorks and fabricated through 3D printing and mold casting. Physical characterization included stress-strain tests, repeatability assessments, and frequency response evaluations. Python is used to process video-tracked strain data and calculate mean and standard deviation across cycles. Different designs are explored in terms of key geometric parameters for bellow-shaped actuators, including multiple tapered edges of 7 and 13, tapered angles of 40° and 60°, and wall thicknesses of 2.5 mm, 3.0 mm, and 3.5 mm, allowing for comparison of actuation performance across configurations. The best-performing design achieved maximum displacement, high strain, and demonstrated strong durability based on repeatability performance, as indicated by a low standard deviation across multiple actuation cycles. The results revealed that design configuration 3 was the most efficient in terms of displacement and structural integrity. Among the thickness variations, Design 1.2 with a 3.5 mm wall thickness exhibited superior performance in structural stability and repeatability. The valuable insight highlighted is that the performance of silicone-based actuators is influenced by geometry and wall thickness, supporting the optimization of soft actuators for precision control and efficiency.

Keywords: *Soft Robotics, Pneumatic Actuator, Silicone Rubber, SolidWorks, Design Optimization*

1.0 INTRODUCTION

The rapid advancements in soft robotics have catalyzed the development of soft pneumatic actuators, particularly for agricultural robotics. These actuators offer adaptability and compliance, making them ideal for handling delicate crops and specialty agricultural products. However, designing actuators capable of precise and adaptive movements remains a critical challenge due to the diverse grasping requirements in agricultural tasks. The dynamic performance characteristics of soft actuators, specifically deformation (measured by maximum displacement) and elongation, combined with the actuator's

thickness, are highly relevant to successful agricultural applications that require the handling of fragile objects. Deformation and elongation are fundamental characteristics that define the "soft" nature of the pneumatic actuator and directly facilitate gentle handling required in agriculture.

Soft pneumatic actuators (SPAs) have been a long-standing and prevalent actuation technology in soft robotics [1], offering significant potential for applications in agriculture due to their safety, durability, ease of fabrication, controllability, low cost, and high lifting weight ratio. These actuators function by applying air pressure to the internal chambers of highly deformable soft materials. Upon inflation, the actuators bend or even grasp due to their structural anisotropy, which favours bending along their low-stiffness direction. The performance of SPAs is evaluated from two perspectives: geometry response, which includes parameters like bending angle and curvature, and mechanical response, which involves measurements of block force and grasping force. It is worth noting that high block force may not always accurately reflect the gripper's actual grasping ability [2], even though it is often correlated with high grasping force. One significant advantage of SPAs is that they do not require heavy equipment or strict operational conditions to generate a relatively large grasping force, as this force is highly proportional to the active air pressure. Most finger grippers constructed using SPAs can achieve a bending angle ranging from 0° to 360°, providing a large workspace for grasping. However, the force response of these actuators can vary significantly depending on the fabrication method and material choice. For example, a high-force soft robotic gripper fabricated using fused deposition modelling 3D-printing technology exhibits a maximum grasping force of approximately 50N, while a similar structure soft pneumatic gripper made from Dragon Skin 30 material demonstrate a maximum pullout force of only 10 N [3].These variations in force response emphasize the importance of carefully selecting the fabrication method and materials when designing SPAs for specific agricultural applications. For instance, in harvesting and picking tasks, such as strawberry or tomato collection, require the highest flexibility and multiple degrees of freedom for soft robotic arms. Fruits are often positioned irregularly among leaves and stems, demanding a manipulator that can bend, twist, and adapt its shape to reach and gently grasp without causing damage.

2.0 RELATED WORKS

Soft actuators are flexible and compliant systems that generate movement through material deformation such as mimicking the properties of biological muscles. It is typically made from soft, elastic materials like silicone and able to operate in various tasks, including gripping, bending, and lifting, depending on the design and application. The main purpose of soft actuators is to transform energy into mechanical movement while maintaining flexibility and do not sacrifice the torque and capability that it can handle. The natural ability of soft robotics can undergo significant and continuous deformations while providing a high degree of freedom compared to rigid robots [4]. Furthermore, the ability to absorb shocks and adapt to environmental changes, is also a key advantage. There are several types of actuation methods identified in these studies for activating the soft actuator, including pneumatic, cable-driven, electroactive polymer, shape memory, electromagnetic, twisted and coiled, and hydraulic systems.

Soft pneumatic actuators can be controlled to enable precise movement which results in deformation by pressurizing chambers using flexible and soft materials like silicone rubber. The design basically relates with actuator materials which allow for smooth and manageable motion and could adapt with various shapes and tasks. These actuators are very suitable for tasks and applications which require high displacement and force such as gripping, lifting, precise positioning and others. Development of a soft gripper for picking and handling delicate fruits, for attaining lower contact pressure and equal distribution of

force around the picked fruit has been one of the proofs that soft pneumatic actuator can handle fragile material [5]. Pneumatic actuation remains the dominant technology in soft robotics due to its light weight, fast response time, and easy implementation [6]. In addition, pneumatic microcontroller systems can be developed using low-cost components such as diaphragm pumps and on/off solenoid valves [7]. Soft robots offer high capability and provide a good safety, large deformations, good power-to-weight ratio [8]. Pneumatic systems also offer smooth control, which is vital for precise and gentle engagement to make it more reliable and prevent damage. Overall, pneumatic actuation provides a robust, efficient, and cost-effective solution for a start-up project to explore the soft robots. Furthermore, in pneumatic actuator, there are some important points that need to be considered which is the shape because the shape of a soft actuator determines its deformation, flexibility, and functionality.

The design of pneumatic soft actuators significantly influences their motion capabilities, controllability, and application potential. Different chamber configurations which are single, double, and triple have been explored to achieve varying deformation modes. The single-chamber design employs only one air chamber, producing unidirectional motion determined by the actuator's geometry. As demonstrated by Sun et al. [9], this design is simple to fabricate, cost-effective, and suitable for preliminary testing. However, due to its asymmetrical structure, its deformation is limited to bending motion, without the capability for elongation or twisting. In contrast, the double-chamber design incorporates two chambers arranged either side-by-side or opposite each other. Pressurizing a single chamber induces bending, whereas simultaneous pressurization of both chambers results in elongation. This configuration offers a balance between motion versatility and control complexity, outperforming single-chamber actuators in deformation capability while being easier to control than triple-chamber designs. Notable implementations include soft grippers and robotic arms developed by Marchese et al. [10] and Shunichi Kurumaya et al. [11]. The three-chamber design consists of three equally spaced air chambers positioned 120° apart, enabling complex multi-directional motions such as bending, twisting, and stretching. Motion is achieved by selectively pressurizing one, two, or all chambers synchronously. To enhance motion precision and structural safety, studies conducted by Qing Xie et al. [12], Gilles Decroly et al. [13] and Yi Sun et al. [14] incorporated threaded fibers into the actuator walls, thereby improving deformation accuracy and reducing the risk of bursting. While this design offers high flexibility and adaptability for advanced soft robotic applications, it requires more sophisticated control systems. The greater the number of chambers pressurized, the lower the pressure required to achieve the same motion. This is because the pressure in each chamber is cumulative, eliminating the need for higher force to produce the same bending curvature at a given angle, particularly at higher pressures [15-16].

3.0 METHODOLOGY

The methodology of this paper is divided into three core phases, which are design, fabrication, and characterisation. In the design phase, actuator geometries were modelled and simulated in SolidWorks. The fabrication phase involved mold printing, silicone casting, and curing. Finally, actuators were tested for displacement, strain, frequency response, and repeatability to evaluate its performance.

3.1 Design of Soft Actuators

The soft actuator design focuses on achieving bending and elongation through pneumatic inflation of internal chambers. Initial hand sketches explored various chamber layouts and geometries to understand motion behavior as shown in Figure 1(i). These ideas were then

developed into detailed CAD models, allowing visualization, dimensioning, and refinement before fabrication. By using SolidWorks, four design variations are created focusing on two pleat types which is section a) 13-pleated consist of Designs 1 and 2 while section b) 7-pleated consist of Designs 3 and 4. Each design varies by pleat angle (60° and 40°) and profile shape to study their effects on deformation and flexibility. The designs share a consistent outer diameter of 26 mm and total height of 60 mm, maintaining a standard scale for comparison during evaluation deformation.as shown in Figure 1(ii). Additionally, Figure 1(iii) describes three identical designs with different wall thicknesses i.e., Thickness 1.0, Thickness 1.1 and Thickness 1.2. These designs share a consistent outer diameter of 26 mm and total height of 60 mm, maintaining a standard scale for comparison during evaluation deformation. These CAD models serve as the basis for both finite element analysis (FEA) and mould fabrication.

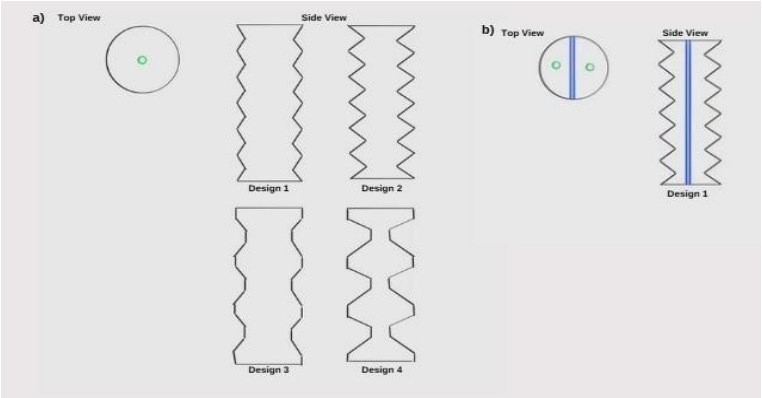

Figure 1(i): Initial hand sketching for (a) Single chamber and (b) Double chamber

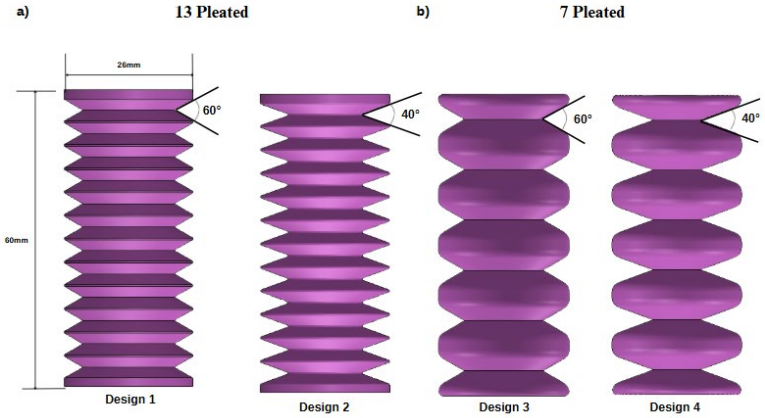

Figure 1(ii): SolidWorks 3D Modeling of Design Variations

The dual internal chamber configuration approach, which is Design 5, is used to evaluate the bending curvature of the soft actuator as shown in Figure 2. Design 5 featuring a dual chamber layout which consists of Chamber 1 and Chamber 2 symmetrically divided along the vertical axis. Each chamber can be pressurized independently from the respective two inlet ports thus enabling control of bending motion depending on which side receives greater pressure. Its geometry applies Design 1's concept which demonstrates how internal reinforcement can modify expansion characteristics and directional bending performance during pneumatic actuation. It offers potential for more complex actuation profiles through

coordinated inflation and a plus point to make it versatile for manipulation and locomotion tasks.

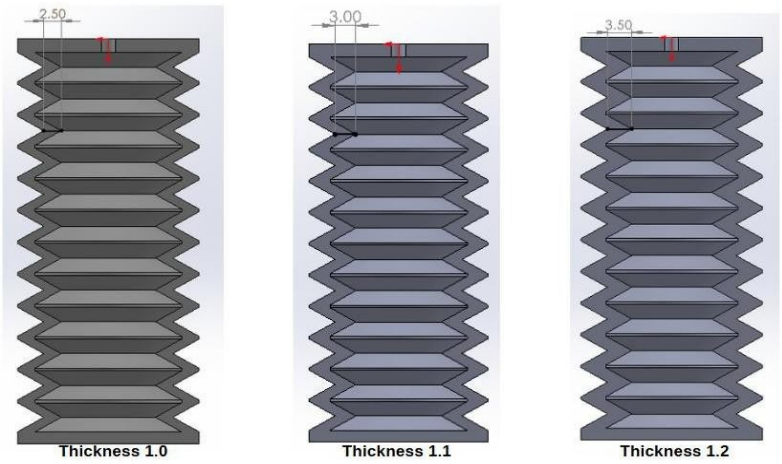

Figure 1(iii): SolidWorks 3D Modeling of Thickness Variations

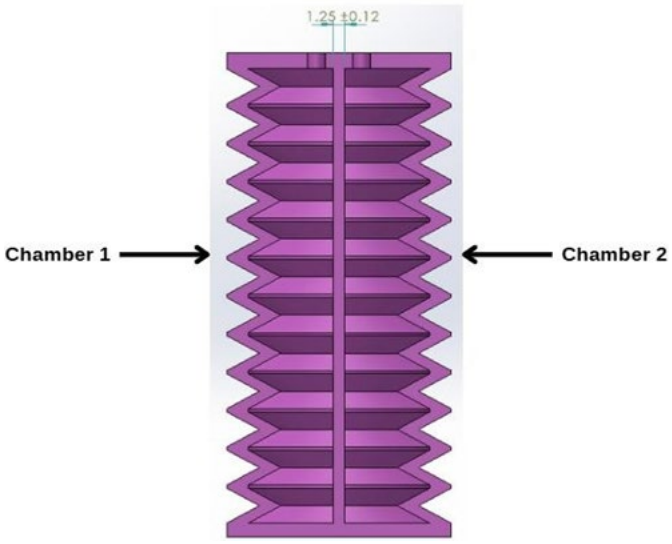

Figure 2: Design 5 with Dual Internal Chambers

3.2 Material Selection

Material selection is crucial to ensure the soft actuator performs reliably. By referring to Table 1, it shows that the specifications of the HL-6 Series Silicone The comparison of the key properties between HL-6 silicone series and Dragon Skin 30 such that, both materials share similar Shore hardness A30 with elongation (~400%), and tear strength, indicating comparable flexibility and durability. HL-6 has a higher viscosity, which may affect injection into the mold but offers greater structural stability. While Dragon Skin 30 exhibits slightly higher tensile strength and offers a longer pot life, HL-6 is more advantageous for rapid prototyping due to its significantly shorter curing time, enabling faster design iteration.

Table 1: Material properties for HL-6 series silicone

Properties	Specifications
Base Viscosity	~50,000 cP
Color	White Translucent
Shore Hardness (A)	A30
Specific Gravity	1.07
Tear Strength	~17 N/mm
Elongation At Break	~400%
Tensile Strength	~3 N/mm²
Pot Life	20 minutes
Cure Time (Full)	12 hours
Flash Point	315.5 °C

3.3 Fabrication Process

Fabricating the soft actuator involves multiple stages including prefabrication, such as mould preparation and silicone preparation. Then, the process proceeds with casting the silicone inside the mould and demould when cured. Lastly, the assembly and bonding process is followed by a finishing stage to remove any residual material and ensure a smooth surface on the prototype. The mould is custom designed for each soft actuator configuration and is utilized in the casting process to fabricate actuators with integrated internal chamber structures essential for pneumatic actuation. Figure 3 highlights the alignment features and cavity design for forming the actuator's internal geometry from top view and front view. It includes a support pillar or guide pin that facilitates precise alignment of the mould halves during the moulding process. Furthermore, at the bottom part, the hole located at the center bottom of the mould serves as the placement point for the syringe used during casting. The adjacent rectangular feature functions as a riser, allowing trapped air bubbles to escape and thereby improving the quality of the final actuator. While the front view illustrates the external form and support features. The two-sided configuration allows for precise alignment during casting, ensuring uniform wall thickness and consistent shape. Top and bottom of mould will produce half of the soft actuator, and the other half needed to do the same before bonding can be applied.

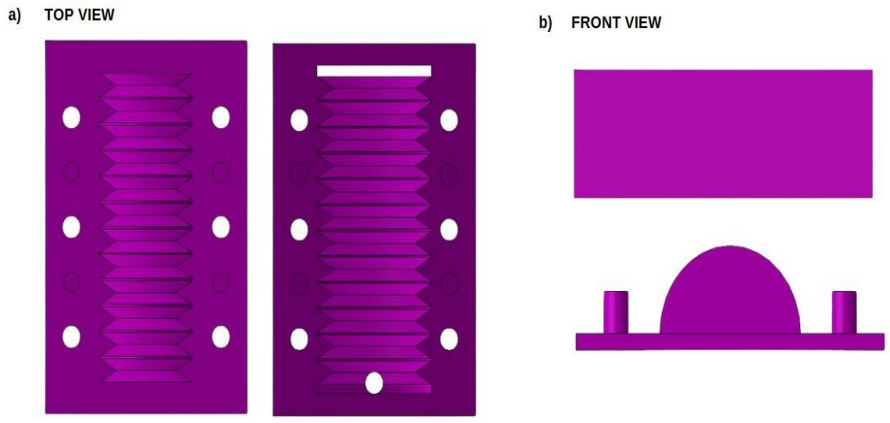

Figure 3: CAD model for mould consist of top and bottom parts

Figure 4 illustrates the silicone casting process used to fabricate the soft actuators. Firstly, materials were measured precisely using a digital scale, targeting a formulation volume of

15 milliliters. The silicone mixture was passed through the vacuum chamber (Figure 5) to remove air bubbles for five minutes, ensuring a defect-free structure. The vacuum is used to eliminate air bubbles form the silicone mixture during the debubbling process which is essential in soft actuators fabrication. This system removes trapped air bubbles that may have formed during the mixing and stirring of Part A and Part B of the silicone actuator in a cup. Once the silicone mixture is placed inside the chamber, the pump reduces the internal pressure, causing the air bubbles to expand and rise to the surface, where they burst and removed from the solution. This method is widely used in research and prototyping environments, particularly in the production of soft actuators, moulds, where precision and material consistency are crucial. Air bubbles can compromise structural integrity, flexibility, and performance of the final cured actuator, making this step critical in ensuring high- quality results. Afterwards, the mixture was loaded into a syringe for precise injection into the 3D-printed mold cavity. Finally, the filled mold was left to be cured at room temperature for 12 hours, solidifying the actuator's shape. This step-by-step process ensures consistent quality in actuator fabrication.

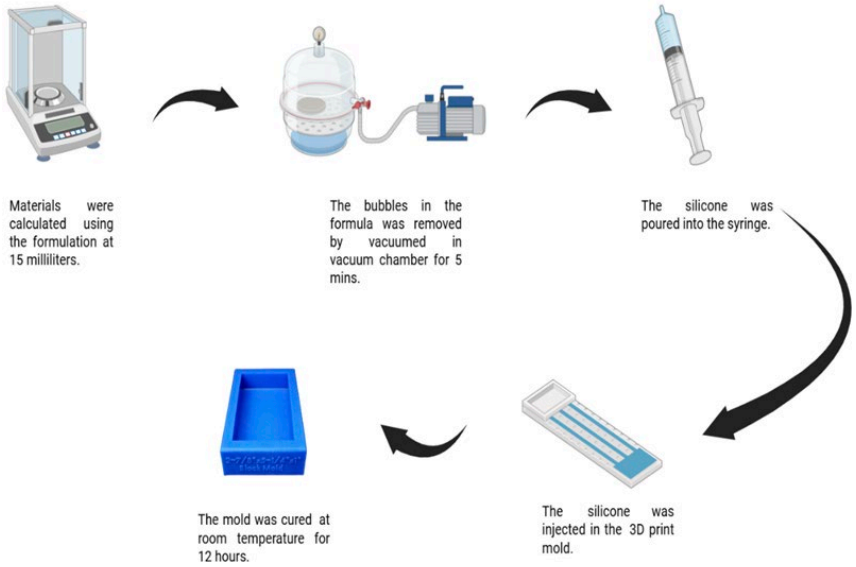

Figure 4: Fabrication Process of Soft Actuator

Figure 5: Process of removing air bubbles from the silicone mixture

Figure 6 demonstrates the casting sequence for a double-chamber soft actuator, requiring three moulds. The first and second moulds are used to fabricate the upper and lower chamber layers respectively. The third mould produces a thin and flat silicone sheet following the pleated design of the actuator that serves as a middle separator between the two chambers as shown in Figure 7. Each part is cast individually by injecting silicone into the respective moulds using syringes.

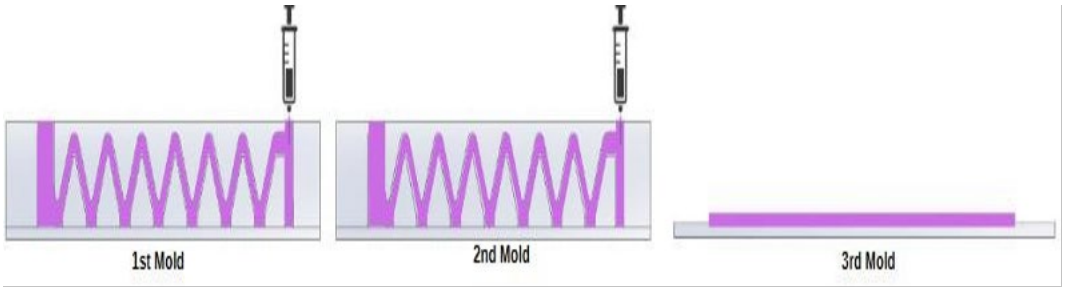

Figure 6: Casting process for double chamber soft actuator

Next, the two chamber layers were bonded using the same silicone material to ensure consistent elongation characteristics. Using different materials is not recommended, as it may compromise the structural integrity at the bonded interface. The red arrows in Figure 7 indicates the bonding surface along the centerline, where adhesive is applied to join the upper and lower silicone structures.

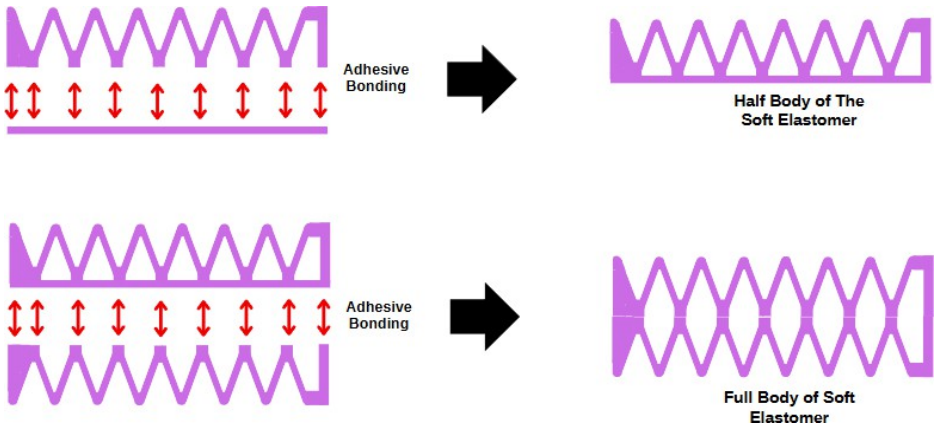

Figure 7: Double chamber design bonding and assembly

Once cured, the two halves become a single integrated soft actuator. This bonding process ensures airtight sealing of internal cavities while preserving flexibility and durability. The bonding process should be performed using the same mould that was used during curing to ensure proper fit and secure attachment. This method is more effective than simply gluing two actuators together without using the mould to apply uniform pressure during bonding. Lastly, tubing ports are being punched at the end of the chamber and sealed with silicone adhesive to make it airtight and prevent leakages from happening and sealed with silicone adhesive to prevent leakage as shown in Figure 8.

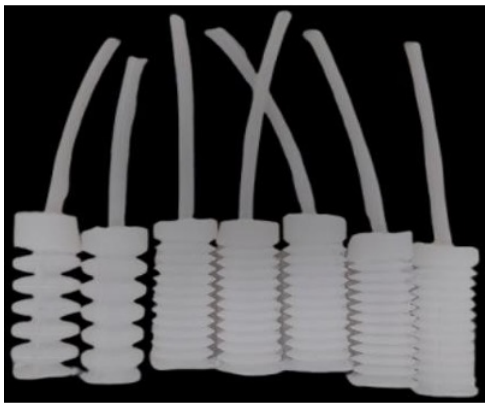

Figure 8: Prototype of completed soft actuators including single and dual chamber designs

3.3 Working Flow of Pneumatic Soft Actuator

The pneumatic soft actuator is designed to perform two key types of deformation which are bending curvature and axial elongation by using pressurized air filled in the chamber. The actuator starts in its neutral or initial shape. When compressed air is introduced into selected internal chambers, it causes the actuator to bend in a specific direction depending on the pressure given. This bending deformation is useful for applications that require directional motion. The pressurized air causes the actuator to stretch vertically, increasing its overall length. This mode is particularly suitable for linear actuation tasks, such as reaching or extending to an object or goals. Both modes rely on the elasticity and flexibility of the silicone material, which allows smooth deformation and recovery.

The actuator is held in place with a rigid holder at the end of it to ensure movement occurs only in the intended directions. This concept allows the soft actuator to mimic biological motion while remaining safe, adaptable, and robust, making it ideal for soft robotic systems. Figure 9 shows the flowchart that illustrates the whole operation of a soft pneumatic actuator, starting from an idle state to controlled deformation via air pressure. The outlines steps will give the process of making the soft actuator from microcontroller activation to valve operation, chamber inflation, deformation, measurement and data collection, forming a repeatable cycle for testing durability, accuracy, and responsive behaviour of the soft actuator.

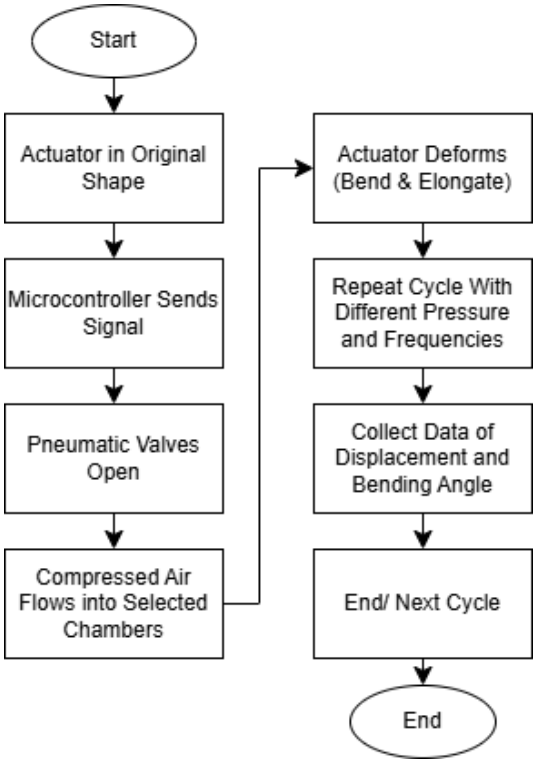

Figure 9: Workflow of the Soft Pneumatic Actuator

4.0 RESULTS AND DISCUSSION

This section presents the evaluation of various soft actuator designs using simulation and experimental testing. It discusses displacement performance, frequency response, repeatability, and bending characteristics across different designs and wall thicknesses. Key findings highlight how design geometry, chamber configuration, and material thickness influence actuator's behaviour, performance, and reliability.

4.1 Simulation Analysis

The analysis begins with simulation studies which include displacement prediction, strain distribution and safety factor evaluation of the actuator when pressurised. Using finite element analysis (FEA) tools in SolidWorks, this study evaluates how actuator geometry, wall thickness, and internal pressure influence deformation or elongation, stress distribution, and overall structural stability. These simulations help identify potential failure points for each actuator to ensure that the design concepts are validated and material

usage is optimized before proceeding to physical fabrication. The color contour in the FEA result illustrates the stress or deformation distribution across the soft actuator when pressure is applied. As the internal pressure is applied, the soft actuator expands unevenly based on its geometry and material properties. The transition of color from blue to red visually represents the gradient of deformation intensity, helping identify which sections of the actuator are most responsive or prone to stress concentration. This analysis is crucial for validating the actuator's design, ensuring uniform deformation and preventing material failure during operation. This simulation compares deformation across four actuator designs as shown in Figure 10. Design 2 shows the highest elongation, while Design 4 reveals structural instability. This analysis helps in identifying the optimal geometry that balances flexibility and safety, with Design 3 showing stable and controlled deformation.

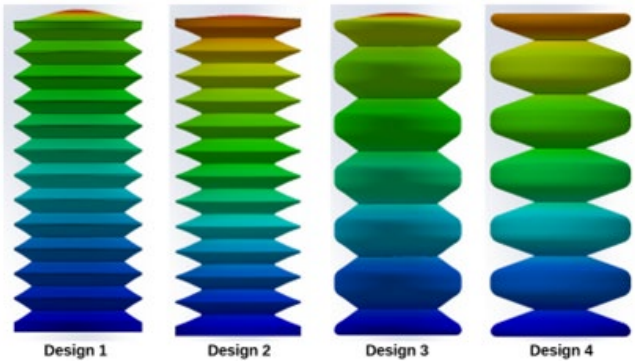

Figure 10: Color Contours with Different Designs (blue = min, red = max)

Additionally, Figure 11 illustrates a simulation to evaluate how different wall thicknesses, i.e., T1.0, T1.1 mm and T1.2, affect actuator deformation. Thinner actuators exhibit higher deformation, however, less structure integrity. In comparison, the actuators with higher wall thickness within the same pressure range show relatively lower deformation, but higher integrity. It validates the trade-off between flexibility and strength in actuator design [16-17].

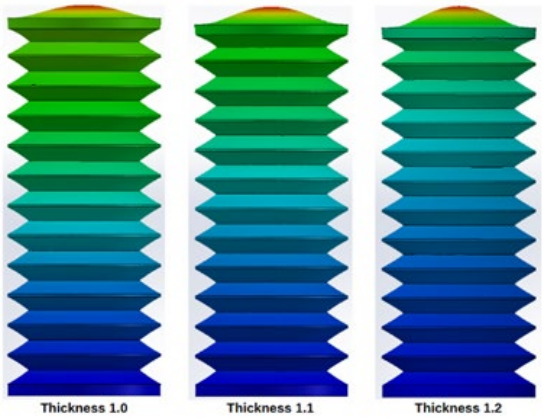

Figure 11: Color Contours with Different Thickness (blue = min, red = max)

Figure 12 shows the bending angle of an actuator with off-centred chamber inflation. The simulation yields a 19.28° deflection, confirming the actuator's directional control

capability. It is crucial for predicting how design affects bending precision in real-world applications like robotic grippers [18-19].

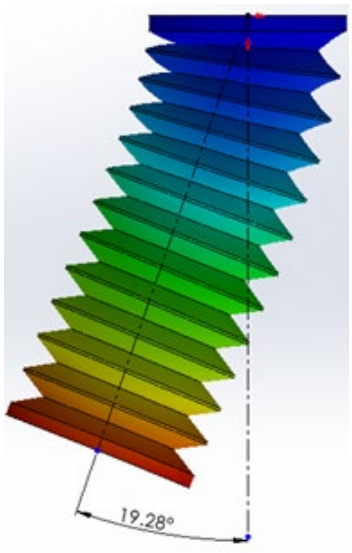

Figure 12: Bending Angle by Actuator of Design 5 with Dual Chamber

In the FEA of a soft actuator, several parameters are evaluated to assess its mechanical performance and reliability under applied pressure. The maximum displacement is obtained from the nodal deformation results, representing the largest movement experienced by any point on the actuator typically shown as the red region in the contour plot. This value indicates the actuator's bending or elongation capability. The strain deformation is determined from the strain tensor calculated by the solver, showing how much the material stretches or compresses during actuation. Areas of high strain are carefully analyzed to identify potential regions of fatigue or material failure. The pressure range is defined through a parametric simulation in which internal pressure is gradually varied to observe its effect on deformation, allowing the determination of an optimal operating pressure that produces sufficient movement without overstressing the material. Finally, the safety factor is computed by comparing the maximum equivalent stress (von Mises) with the material's yield strength, ensuring the actuator remains within safe limits during operation. Collectively, these analyses validate the actuator's design performance, optimize material use, and ensure durability before physical fabrication.

Structural variations significantly influence deformation in terms of bending response under positive pressure, where a larger pressurizable gas area leads to greater deformation, as demonstrated by Hao et al. [20]. Design 2 exhibits the highest displacement, indicating superior elasticity, followed by Design 4 as shown in Figure 13. Designs with thicker walls, which are Thickness 1.2, show lower displacement, highlighting the trade-off between strength and flexibility.

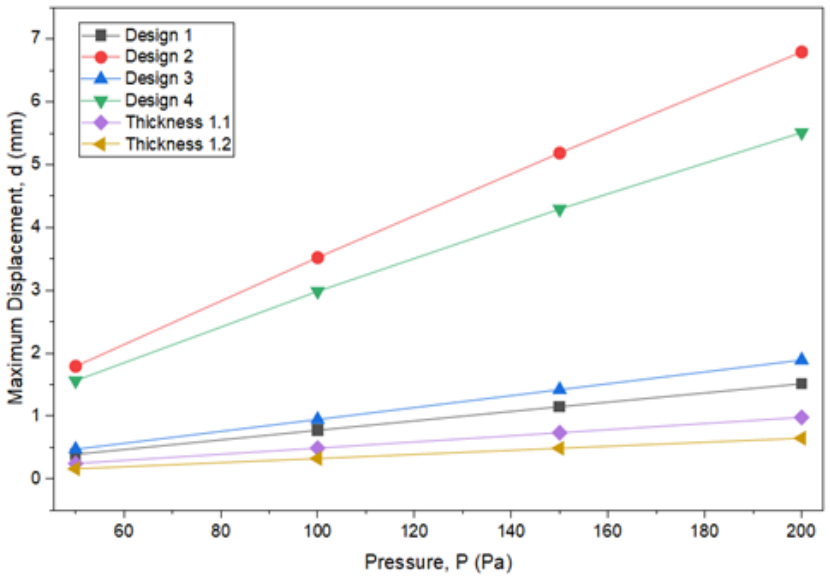

Figure 13: Graph of Maximum Displacement vs Pressure

Similarly, Figure 14 shows strain results that mirror the displacement trend, with Design 2 achieving the highest strain values, confirming its high deformability. Thicker actuators show lower strain, indicating stiffer structures. This graph supports material and geometric optimisation for desired actuator performance in soft robotics.

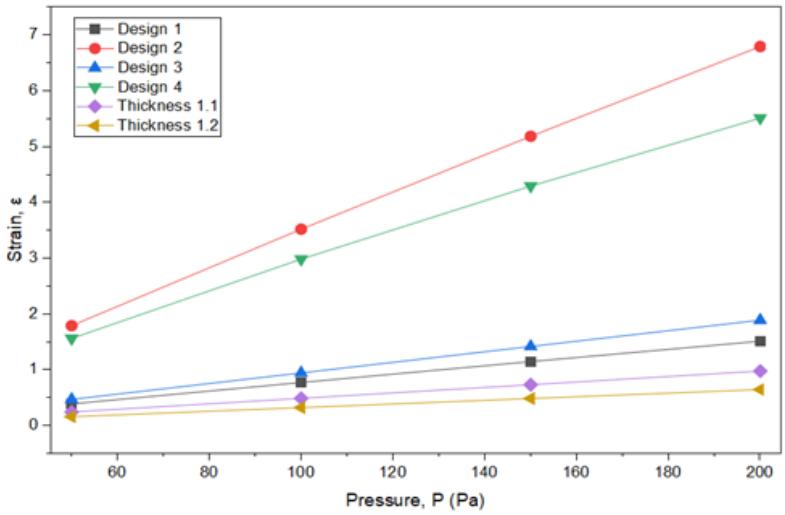

Figure 14: Graph of Strain vs Pressure

Table 2 describes that Design 3 and Thickness 1.2 have the highest safety factor and maximum pressure capacities, indicating strong structural integrity. Meanwhile, Design 2 has the lowest safety factor, suggesting limited durability. Higher safety factor correlates with better material distribution and geometry, making these designs more reliable for high-pressure soft robotic applications.

Table 2: Safety Factor and Maximum Pressure Applicable

Actuators	Safety Factor at 200 Pa	Maximum Pressure (kPa)
Design 1	690.6	138.1
Design 2	348.0	69.00
Design 3	794.2	158.8
Design 4	414.8	83.0
Thickness 1.1	748.7	149.5
Thickness 1.2	838.7	167.7

4.2 Physical Characterisation of Soft Actuator

This section evaluates the real-world performance of soft actuators through displacement, bending angle, and repeatability tests. Each design and thickness variation were tested under different pressures and frequencies. Various tests were performed to get the overall behaviour of the actuator such as pressure vs displacement, repeatability under cyclic pressure, frequency response and configurations for number of chambers being pressurised. The motion data was extracted using video tracking software known as Tracker, prior using Excel for data collection. Furthermore, python was used to obtain the graph of average and standard deviation for evaluation from the command. The experiments were conducted to measure maximum displacement (strain), bending angle, repeatability with 5 cycles of testing, and frequency response of 1 Hz, 5 Hz and 20 Hz. The system connects to the actuator via a tube and delivers controlled air pressure from a compressor. The USB and serial connections enable the box to be operated using a Python script which automates test parameters like frequency and pressure cycles of the actuator. This interface is essential to enable reliable comparison across different actuator designs and configurations tested throughout this study. Figure 15 illustrates the experimental setup.

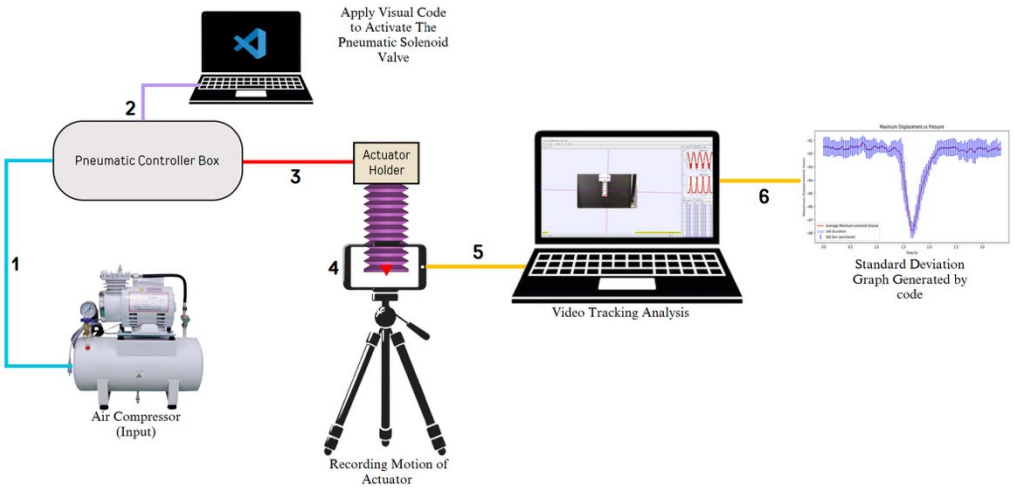

Figure 15: Overall Experimental Testing Workflow for Mechanical Performance Evaluation.

4.2.1 Maximum Displacement

The performance of single and double chamber actuators is compared in terms of elongation when both chamber are actuate at the same time with the same pressure for

chamber 1 and 2 while bending angle produce will be compared with the simulation to prove that the simulation accuracy is at certain level that can be useful especially to get the overall view on how the actuator will act under certain pressure. These tests provide a comprehensive understanding of the actuator's mechanical response behaviour, consistency, and adaptability. Figure 16 visually compares the maximum elongation of four actuator designs under pneumatic pressure, highlighting structural differences and deformation performance. It supports quantitative data by showing physical shape changes, validating displacement results, and helping to evaluate the influence of geometry on actuation efficiency and structural stability during inflation.

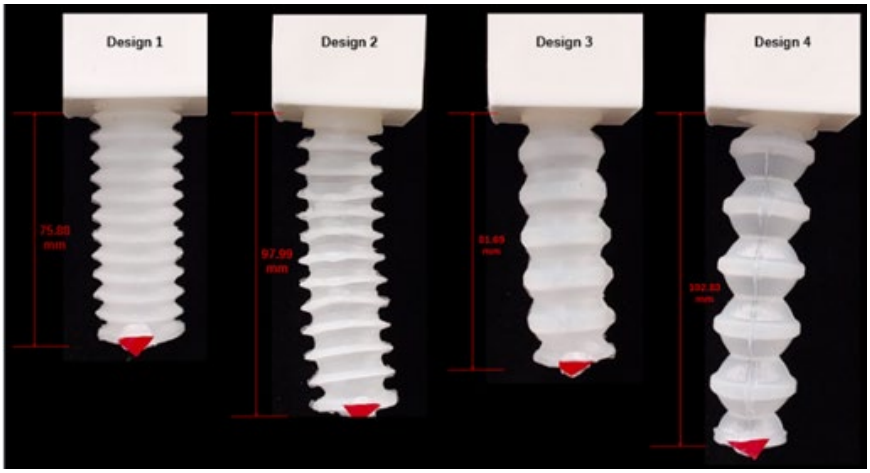

Figure 16: Maximum Displacement for single chamber designs.

Figure 17 demonstrates the effect of varying wall thicknesses on actuator elongation under the same pressure. This result validates how material stiffness influences deformation, showing that increased thickness slightly reduces displacement as the structure become more rigid, which is important for optimizing durability and performance in soft actuator design [21].

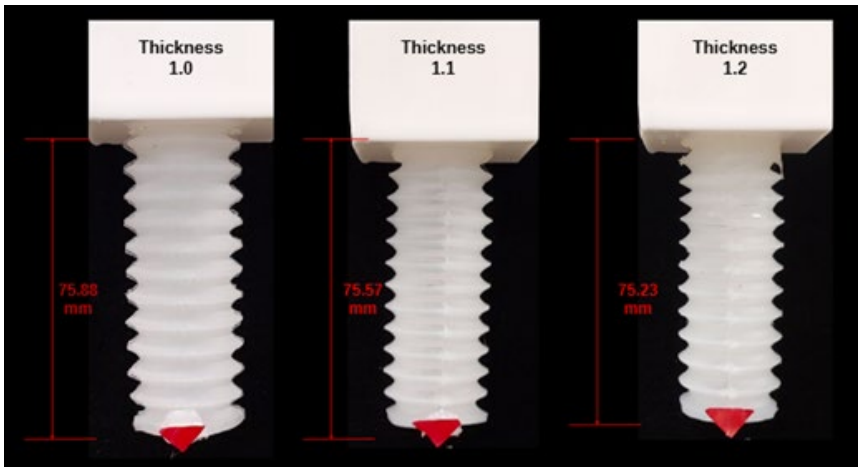

Figure 17: Effect of Wall Thickness on Maximum Displacement

Table 3 shows that at 48 kPa, increasing wall thickness results in lower maximum displacement, indicating reduced flexibility. However, at 34 kPa, displacement remains

approximately consistent across all thicknesses, suggesting wall stiffness as a less effective factor under lower pressure conditions. While the displacement at lower pressure, which is 34 kPa is not significantly different because the force generated is insufficient to fully engage the material stiffness differences. At this lower pressure, all actuator walls regardless of thickness deform similarly, resulting in minimal variation in displacement. The material's elastic limit isn't fully challenged.

Table 3: Maximum Displacement at 48 kPa and 34 kPa

Actuators	Max. Displacement at 48 kPa (mm)	Max. Displacement at 34 kPa (mm)
Design 1	89.89	75.88
Design 2	102.95	97.99
Design 3	88.21	81.69
Design 4	80.53 (Fail)	102.83
Thickness 1.1	73.93	75.57
Thickness 1.2	70.64	75.23

4.2.2 Repeatability Test

This analysis is crucial in determining which design offers reliable and repeatable actuation where the nature of soft robot that act as actuator and will be applied many cycles during its operation where consistent deformation is essential for controlled motion. Table 4 shows that this test is essential to evaluate the repeatability and reliability of actuator performance. Design 3 demonstrated the lowest standard deviations, indicating highly consistent motion. Despite slightly lower displacement, their stable output makes them ideal for precise, controlled soft robotics applications where repeatable performance is critical.

Table 4: Different Design Actuators of Average Displacement and Standard Deviation (STD)

Actuator Design	D1	D2	D3	D4
Cycle 1 (mm)	76.49	99.15	82.10	103.33
Cycle 2 (mm)	76.64	98.84	81.66	103.24
Cycle 3 (mm)	75.86	97.75	81.62	103.20
Cycle 4 (mm)	75.82	97.15	81.61	102.41
Cycle 5 (mm)	74.60	97.07	81.46	101.98
Avg. Displacement (mm)	75.88	97.99	81.69	102.83
STD. (mm)	0.72	0.86	0.22	0.54

Table 5 shows that repeatability tests using standard deviation from five actuation cycles demonstrated that Thickness 1.2 exhibited the least variation (±0.12 mm), indicating consistent mechanical behavior under repeated stress. Frequency response testing showed that actuators generally performed better at lower frequencies of 1 Hz, with displacement reducing at higher actuation speeds due to material damping.

Table 5: Different Thickness Actuators of Average Displacement and Standard Deviation (STD)

Actuator Thickness	T1.0	T1.1	T1.2
Cycle 1 (mm)	76.49	99.15	82.10
Cycle 2 (mm)	76.64	98.84	81.66
Cycle 3 (mm)	75.86	97.75	81.62

Cycle 4 (mm)	75.82	97.15	81.61
Cycle 5 (mm)	74.60	97.07	81.46
Avg. Displacement (mm)	75.88	97.99	81.69
STD. (mm)	0.72	0.86	0.22

4.2.3 Frequency Response Test

Frequency response test represents the rate at which the actuation signals are passed to the soft actuator. At 1 Hz, the steps of pressure signals are one second apart, allowing the actuation chamber to inflate properly. Similarly, at 10 Hz, the pressure steps are 0.1 seconds apart, giving less time to the actuator chamber to fill up with the pressure. This behavior results in fast actuator movements, introducing more dynamic behaviors as demonstrated in [19]. Testing at different frequencies helps evaluate the actuator performances under varying speeds of operation, identifying potential issues such as material lag, hysteresis or reduced displacement due to fast actuation [22].

Figure 18 visually demonstrates the effect of actuation frequency on Design 3's displacement. As frequency increases from 1 Hz to 20 Hz, the actuator extension decreases from 81.69 mm to 69.73 mm. This confirms that higher frequencies reduce displacement due to insufficient inflation time during faster cycles.

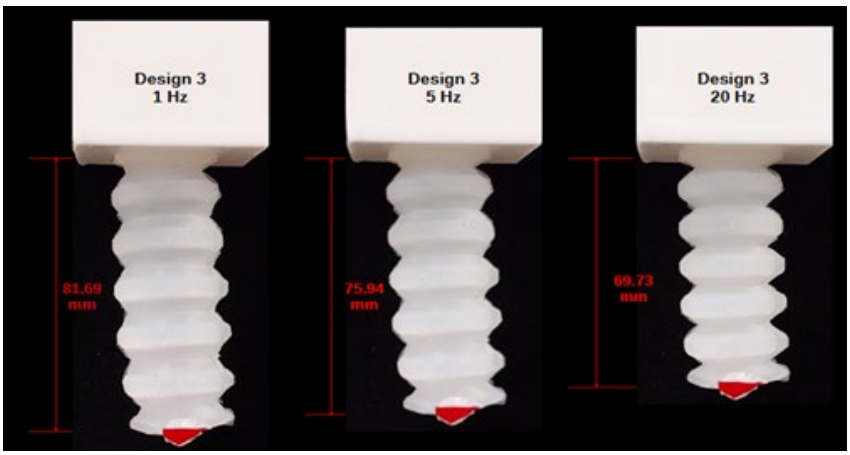

Figure 18: Deformation of Actuator Design 3 with Various Frequencies

Table 6 presents frequency test is significant to assess actuator responsiveness at varying input speeds. The table shows a clear trend which results in frequency increasing from 1 Hz to 20 Hz, maximum displacement consistently decreases across all designs and thicknesses. This indicates that higher frequencies reduce the time available for full inflation, limiting actuator extension and affecting performance, signifying the optimal rate of actuation for application purposes and requiring sophisticated controllers for robotic applications with desired precision as demonstrated in [17, 23].

Table 6: Maximum Displacement Across All Type of Actuators

Actuator	Max. Displacement (mm)		
	1 Hz	5 Hz	20 Hz
Design 1	75.88	72.34	68.09
Design 2	97.99	88.79	76.90

Design 3	81.69	75.94	69.73
Design 4	102.83	96.39	83.803
Thickness 1.1	75.57	73.13	68.32
Thickness 1.2	75.23	72.60	67.43

4.2.4 Single Versus Double Chamber Configuration

The pressure-chamber relationship plays a pivotal role in optimizing soft pneumatic actuator performance. A deep understanding of this relationship enables the development of tailored characterization protocols that align with specific design requirements. By strategically determining the number and configuration of chambers, prototypes can be engineered to achieve targeted motion profiles and enhanced efficiency, thereby advancing the state-of-the-art in soft actuator design. Based on Figure 19, it shows that Design 5 exhibits slightly lower displacement which is 74.35 mm compared to Design 1 with 75.88 mm of maximum elongation due to its internal structure featuring two chambers separated by a central vertical wall with 1.25 mm thickness.

This added internal partition increases stiffness and limits expansion, making the actuator more rigid. While this configuration may improve structural strength and durability, it reduces overall flexibility and elongation under pressure, highlighting a trade-off between stability and deformation capability in soft actuator design [7].

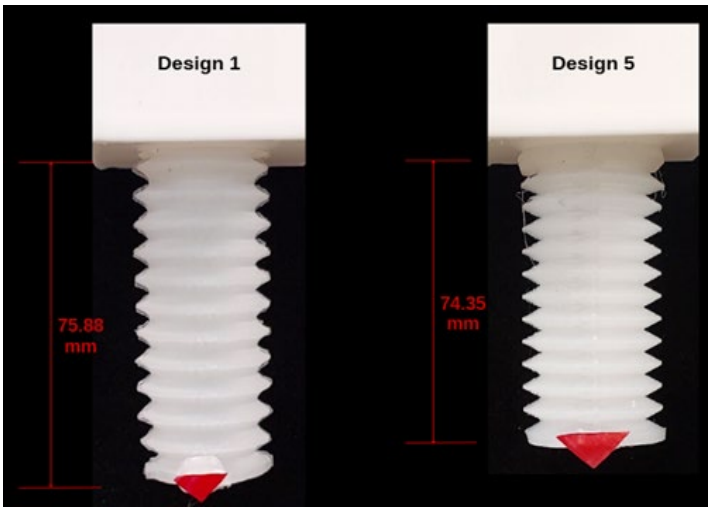

Figure 19: Max. Displacement Between Design 1 and Design 5

Table 7 compares the performance of Design 1 and Design 5 actuators with different chamber configurations. Design 1 has a single chamber with 34 kPa, while Design 5 has two chambers with 17 kPa each. Despite the lower pressure per chamber, Design 5 achieves similar displacement to Design 1 across all frequencies, indicating improved efficiency and structural optimisation due to dual-chamber distribution.

Table 7: Maximum Displacement Between D1 and D5 with Varies Frequencies

Actuator		D1	D5
No. of Chamber Configurations		1	2
Pressure Applied (kPa)		34	17
Max. Displacement (mm)	**1 Hz**	75.88	74.35
	5 Hz	72.34	72.47
	20 Hz	68.09	67.92

Figure 20 illustrates the bending angles of Design 5 at different actuation frequencies. As frequency increases from 1 Hz to 20 Hz, the bending angle decreases from 21.7° to 16.2°, indicating reduced deformation. This trend highlights the frequency-dependent performance of the actuator, crucial for applications requiring precise motion control under varying input rates [17,23].

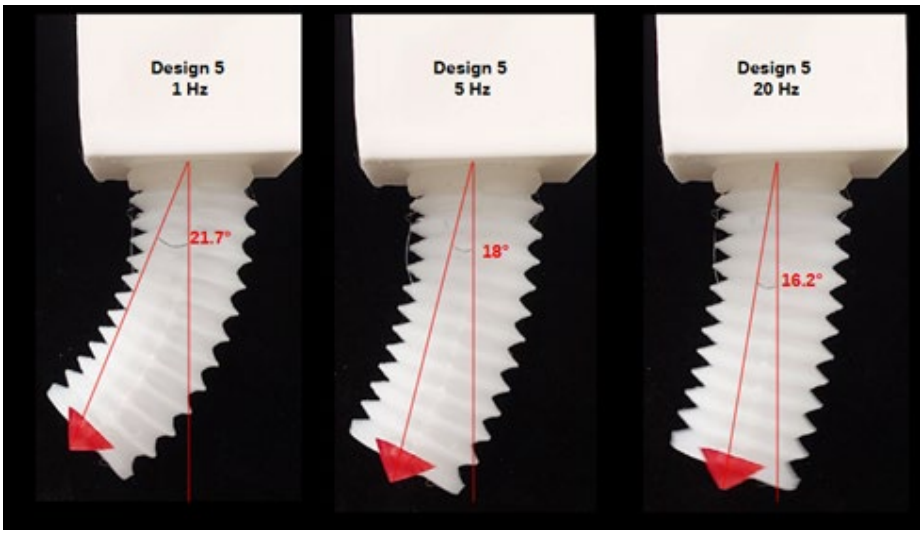

Figure 20: Bending Angle for Design 5 with Varies of Frequencies

Table 8 was collected to evaluate how individual chamber inflation affects directional bending in Design 5 under varying frequencies. Chamber 2 consistently produced higher bending angles than Chamber 1 due to its orientation and less stiffness, while Chamber 1's central wall thickness of 1.25 mm contributed to reduced deformation. Fabrication inconsistencies such as uneven curing, trapped air bubbles, or mold misalignment may also have caused stiff differences between chambers, introducing uncertainty in actuator response across multiple fabrication instants as demonstrated in [22]. These results highlight that both internal design and fabrication quality significantly impact the actuator's motion and are critical for achieving precise, repeatable control in multi-chamber soft robotic systems.

For future work, improvements in fabrication precision using high-resolution 3D-printed moulds are recommended to control wall thickness more accurately [8,19]. Embedding flexible sensors can enable real-time feedback and closed-loop control [21]. Expanding to multi-chamber and multi-actuator systems may allow for more complex motions and broader applications in adaptive grippers, wearable robotics, and advanced soft robotic system [24-25].

Table 8: Maximum Bending Angle Between 2 Chambers of Design 5

Actuator		D5	D5
No. of Chamber		Chamber 1	Chamber 2
Pressure Applied (kPa)		34	17
Max. Bending Angle (degrees)	1 Hz	75.88	74.35
	5 Hz	72.34	72.47
	20 Hz	68.09	67.92

5.0 CONCLUSION AND RECOMMENDATION

This study successfully achieved its objective of designing, fabricating, and characterizing soft pneumatic actuators with variations in design, wall thickness, and chamber configuration. SolidWorks simulations and physical testing validated the actuator performance in terms of displacement, repeatability, and structural integrity. Among the tested models, Design 3 emerged as the most efficient, demonstrating a high safety factor, maximum displacement of 88.2 mm at 48 kPa, and excellent repeatability with a standard deviation of 0.22 mm, indicating reliable performance under cyclic actuation. In contrast, Design 4 showed the highest displacement at low pressure but failed structurally at high pressure, highlighting the trade-off between flexibility and durability for a given material. Similarly, Thickness 1.2 exhibited the best repeatability but lower displacement, while Thickness 1.0 offered high deformation with lower consistency. These findings emphasize how geometry and material parameters influence actuator's behaviour and performance.

ACKNOWLEDGEMENT

The authors would like to thank The Soft Robotic Lab, National University of Singapore (NUS) for their helpful feedback and support in conducting testing and experiments.

REFERENCES

1. Xavier, L. D. Silva, R. de Lima, and M. Silva, "Advances in soft robotics for medical applications," Journal of Medical Robotics Research, vol. 7, no. 2, pp. 101-114, 2022.
2. Y. Sun, X. Li, H. Zhang, and Q. Liu, "Recent advances in soft robotics and their applications," Soft Robotics, vol. 9, no. 5, pp. 624-639, 2022.
3. Y. Liu, J. Hou, C. Li, and X. Wang, "Intelligent Soft Robotic Grippers for Agricultural and Food Product Handling: A Brief Review with a Focus on Design and Control," Advanced Intelligent Systems, vol. 5, no. 1, p. 2300233, 2023. https://doi: 10.1002/aisy.202300233
4. Yuxuan, W., Wang, J., & Fei, Y. (2021). Design and Modeling of Tetrahedral Soft- Legged Robot for Multigait Locomotion. IEEE/ASME Transactions on Mechatronics, PP, 1–1. https://doi.org/10.1109/TMECH.2021.3087611
5. Venter, D., & Dirven, S. (2017). Self-morphing soft-robotic gripper for handling and manipulation of delicate produce in horticultural applications. 2017 24th International Conference on Mechatronics and Machine Vision in Practice (M2VIP), 1–6. https://doi.org/10.1109/M2VIP.2017.8211516
6. Dou, W., Zhong, G., Cao, J., Shi, Z., Peng, B., & Jiang, L. (2021). Soft Robotic Manipulators: Designs, Actuation, Stiffness Tuning, and Sensing. Advanced Materials Technologies, 6(9), 2100018. https://doi.org/10.1002/admt.202100018
7. Santoso, J., Skorina, E. H., Salerno, M., de Rivaz, S., Paik, J., & Onal, C. D. (2019). Single chamber multiple degree-of-freedom soft pneumatic actuator enabled by adjustable stiffness layers. *Smart materials and structures*, *28*(3), 035012.

8. Tawk, C., & Alici, G. (2021). A review of 3D-printable soft pneumatic actuators and sensors: Research challenges and opportunities. Advanced Intelligent Systems, 3(6), 2000223. https://doi.org/10.1002/aisy.202000223
9. Sun, E., Wang, T., & Zhu, S. (2020). An experimental study of bellows-type fluidic soft bending actuators under external water pressure. Smart Materials and Structures, 29(8), 087005. https://doi.org/10.1088/1361-665X/ab9518
10. Marchese, A. D., Katzschmann, R. K., & Rus, D. (2015). A Recipe for Soft Fluidic Elastomer Robots. Soft Robotics, 2(1), 7–25. https://doi.org/10.1089/soro.2014.0022
11. Kurumaya, S., Phillips, B. T., Becker, K. P., Rosen, M. H., Gruber, D. F., Galloway, K. C., Suzumori, K., & Wood, R. J. (2018). A Modular Soft Robotic Wrist for Underwater Manipulation. Soft Robotics, 5(4), 399–409. https://doi.org/10.1089/soro.2017.0097
12. Xie, Q., Wang, T., Yao, S., Zhu, Z., Tan, N., & Zhu, S. (2020). Design and modeling of a hydraulic soft actuator with three degrees of freedom. Smart Materials and Structures, 29(12), 125017. https://doi.org/10.1088/1361-665X/abc26e
13. Decroly, G., Lambert, P., & Delchambre, A. (2021). A Soft Pneumatic Two-Degree-of-Freedom Actuator for Endoscopy. Frontiers in Robotics and AI, 8. https://doi.org/10.3389/frobt.2021.768236
14. Sun, Y., Song, S., Liang, X., & Ren, H. (2016). A Miniature Soft Robotic Manipulator Based on Novel Fabrication Methods. IEEE Robotics and Automation Letters, 1(2), 617–623. https://doi.org/10.1109/LRA.2016.2521889
15. Chen, Y., Zhang, J., & Gong, Y. (2019). Utilizing anisotropic fabrics composites for high-strength soft manipulator integrating soft gripper. *IEEE Access, 7*, 127416–127426. https://doi.org/10.1109/ACCESS.2019.2940499
16. Shintake, J., Rosset, S., Schubert, B., Floreano, D., & Shea, H. (2016). Versatile soft grippers with intrinsic electroadhesion based on multifunctional polymer actuators. *Advanced Materials, 28*(2), 231–238. https://doi.org/10.1002/adma.201504264
17. Nazeer, M. S., Laschi, C., & Falotico, E. (2023). Soft DAgger: Sample-efficient imitation learning for control of soft robots. *Sensors, 23*(19), 8278. https://doi.org/10.3390/s23198278
18. Park, Y.-L., Santos, J., Galloway, K. G., Goldfield, E. C., & Wood, R. J. (2014). A soft wearable robotic device for active knee motions using flat pneumatic artificial muscles. *2014 IEEE International Conference on Robotics and Automation (ICRA)*, 4805–4810. https://doi.org/10.1109/ICRA.2014.6907562
19. Zhang, X., Pan, T., Heung, H. L., Chiu, P. W. Y., & Li, Z. (2018). A biomimetic soft robot for inspecting pipeline with significant diameter variation. *2018 IEEE/RSJ International Conference on Intelligent Robots and Systems (IROS)*, 7486–7491. https://doi.org/10.1109/IROS.2018.8594390
20. Hao, Y., Wang, T., Ren, Z., Gong, Z., Wang, H., Yang, X., ... & Wen, L. (2017). Modeling and experiments of a soft robotic gripper in amphibious environments. *International Journal of Advanced Robotic Systems*, *14*(3), 1729881417707148.
21. Caasenbrood, B., Pogromsky, A., & Nijmeijer, H. (2024). Sorotoki: A MATLAB toolkit for design, modeling, and control of soft robots. *IEEE Access*. Advance online publication. https://doi.org/10.1109/ACCESS.2024.3357351
22. Nazeer, M.S., Zaidi, S.S.Z., Cianchetti, M. and Falotico, E., 2024, December. Inherent behavioral stochasticity in soft robots: Analysis and control strategies. In IOP Conference Series: Materials Science and Engineering (Vol. 1321, No. 1, p. 012009). IOP Publishing.
23. Nazeer, M.S., Laschi, C. and Falotico, E., 2024. Rl-based adaptive controller for high precision reaching in a soft robot arm. IEEE Transactions on Robotics, 40, pp.2498-2512.
24. Wei, F., Luo, K., Zhang, Y., & Jiang, J. (2024). Structural design and kinematic analysis of cable–driven soft robot. *Actuators, 13*(12), Article 12. https://doi.org/10.3390/act13120497
25. Terkildsen, M., & Rus, D. (2022). Soft robots that self-heal after damage. *Science Robotics, 7*(68), eabn6910. https://doi.org/10.1126/scirobotics.abn6910